Feasibility of an evolutionary artificial intelligence (AI) scheme for modelling of load settlement response of concrete piles embedded in cohesionless soil

Ameer A. Jebur[a, *], William Atherton[b], and Rafid M. Al Khaddar[b]

[a] Department of Civil Engineering, Liverpool John Moores University, Henry Cotton Building, Webster Street, Liverpool L3 2ET, UK.
[b] Department of Civil Engineering, Liverpool John Moores University, Peter Jost Centre, Byrom Street, Liverpool L3 3AF, UK.
[*]E-mail: A.A.Jebur@2015.ljmu.ac.uk; ameer_ashour1980@yahoo.com, Tel.: +0044-7435851479

Abstract

This investigation aimed to examine the load carrying capacity of model piles embedded in sand soil and to develop a predictive model to simulate pile settlement using a new artificial neural network (ANN) approach. A series of experimental pile load tests were carried out on model concrete piles, comprised of three piles with slenderness ratios of 12, 17 and 25. This was to provide an initial dataset to establish the ANN model, in attempt at making current, in situ pile-load test methods unnecessary. Evolutionary Levenberg-Marquardt (LM) MATLAB algorithms, enhanced by T-tests and F-tests, were developed and applied in this process. The model piles were embedded in a calibration chamber in three densities of sand; loose, medium and dense. According to the statistical analysis and the relative importance study, pile lengths, applied load, pile flexural rigidity, pile aspects ratio, and sand-pile friction angle were found to play a key role in pile settlement. Results revealed that the optimum model proposed algorithm precisely characterised pile settlement. There was close agreement between the experimental and predicted data (Pearson's R = 0.988, P = $6.28*10^{-31}$) with relatively insignificant root mean square error (RMSE) of 0.002.

Keywords: Levenberg-Marquardt MATLAB algorithm; pile load-settlement; sandy soil; pile slenderness' ratio; sand relative density.

1. Introduction

Pile foundations are slender structural elements situated beneath superstructures, frequently used as soil settlement controls and load transferring systems at sites where there are inadequate sub-soil layers. Pile foundations are the most acceptable and reliable solution to support and deliver the required structural integrity and serviceability for

offshore structures supported by pile foundations, i.e. wind turbine, gas and oil platforms (Doherty et al. 2015). The safety requirements when designing offshore structures has been cited by many scholars as a significant concern for offshore operating companies (Elsayed et al. 2014) making the accurate determination of pile bearing capacity and settlement under working loads of these structures is of great importance. In marine structures, piles transfer applied loads through a combination of end bearing and mobilised shaft resistance developed within the contact soil in the effective stress zone (Jebur et al. 2016). Where uplift loads govern the foundation design process, mobilised skin friction resistance becomes the main factor that contributes to the pile bearing capacity (Fattah and Al-Soudani 2016). Thus , piles need to be driven deeper than those only subjected to axial compression loads in order to achieve adequate mobilised resistance (Tomlinson and Woodward 2014). It has been documented by Das (2015) that pile bearing capacity can be calculated by dividing the ultimate applied load by a specific factor of safety, taking into consideration the structure strength and its serviceability. Associated pile settlement, on the other hand, can be probably attributed as a consequence of an increase in effective stress, resulting in elastic compression and a reduction in soil volume in the effective stress zone.

In conventional procedures, pile settlement can be determined by dividing the sub-soil profile into different sections. The total summation of the compression in soil layers is equal to the settlement (Tomlinson and Woodward 2014). Uncertainties and preconditions associated with a range of factors, including soil stress history, soil stress history, nonlinear relationships between soil stress-strain and stress distribution due to sampling, have been cited as barriers to precisely calculating pile bearing capacity and associated pile settlement (Loria et al. 2015). Therefore, there has recently been increase in the number of experimental and numerical studies concerning pile-bearing capacity (Xu et al. 2013; Kaiser and Snyder 2014; Sui et al. 2016). However, for the sake of simplification and by necessity, several hypotheses associated with the significant parameters that govern pile settlement have been assumed. This has resulted in the fact that the majority of current approaches fail to provide a comprehensive methodology with continuous degree of success with respect to pile settlement.

In-situ tests, such as dynamic load tests, static pile load tests, standard penetration tests, and cone penetration tests are the most common methods to provide a full detail of pile capacity and its settlement. Nevertheless, while essential, the aforementioned approaches come with their own difficulties in that they are being expensive, tedious, and time consuming, present complications for the construction process, and are not environmentally

friendly (Momeni et al. 2014). Therefore, searching for efficient, accurate and reliable technique to capture the full response of pile load-settlement curve is inevitable.

There are situations where computational intelligence (CI), based on artificial neural networks (ANNs), has been introduced and found to be a more robust and accurate approach in comparison to other modelling methods (Alkroosh and Nikraz 2014). ANN is a bio-inspired system utilise to mimic the biological topology of the human brain and nervous system (Schmidhuber 2015). The work reported in this paper is inspired by the successful applications of artificial intelligence (AI) technology in different ranges of engineering problems, such as, materials modelling (Mohammadi and Ashour 2016) hydrologic and hydraulic modelling problems (Kabiri-Samani et al. 2011; Jaeel et al. 2016) offshore structures implementation (Kabiri-Samani et al. 2011), and geotechnical modelling (Alkroosh and Nikraz 2014), etc. it should be noted that there are other modelling approaches based on soft machine learning concept such as the Moving Least Square (MLS) method, which has been successfully applied in simulating the complex materials behaviour (Vu-Bac et al. 2014).

Recently, the feasibility of artificial neural networks (ANN) applications have been successfully applied in a wide range of geotechnical engineering modelling problem, giving acceptable levels of accuracy (Alkroosh et al. 2015; Ebrahimian and Movahed 2016). Ismail and Jeng (2011) applied a higher order neural network model to estimate the load-settlement behaviour of model piles subjected to axial loading. Two hidden layers, with 14 input parameters, were used to train the optimum topology of the adopted network. Pile characteristics and a standard penetration test (SPT) were entered in the input space to develop and train the proposed network. In another study, Ismail et al. (2013) utilised a soft computing tool to model the pile load-deformation response using an optimised artificial intelligence (AI) approach enhanced with particle swarm optimisation (PSO). This model was developed and trained using pile load test data for model piles, embedded in cohesive and non-cohesive soil. The performance of the trained model was assessed using two indicators; a correlation coefficient (R) and root mean square error (RMSR). The results demonstrated that both models had the ability to predict pile load-settlement with acceptable degrees of accuracy. The study presented in this paper is different from the aforementioned predictive models in two aspects. Firstly, a comprehensive statistical analysis was conducted before the network training process, to identify the most influential individual variables (IVs) to be used in the input layer space, to examine the reliability of the proposed dataset and to mark the level of contribution of each IV on the study outcomes. Secondly, a novel, self-tuning Levenberg-Marquardt scheme, trained with five relatively simple input parameters, enriched with

Hypothesis testing (T-tests and F-tests) was implemented. Unlike traditional ANN training systems, the aforementioned algorithm has several positive features in that it is easy to utilise, self-tuning (does not include user dependent parameters), less vulnerable to overfitting phenomena, faster, and more reliable than other back-propagation (BP) approaches (Hagan and Menhaj 1994; Abdellatif et al. 2015).

Fattah and Al-Soudani (2014) studied the influence of soil plugs on the pile bearing capacity of steel piles placed in loose sand. Different parameters were included in the testing programme, including pile slenderness ratio, method of pile installation and soil plug removal with respect to plug length. The results revealed that pile-bearing capacity was highly influenced by the percentage of plug soil and pile geometry. In addition, Fattah et al. (2016) conducted another experimental study to estimate the pile bearing capacity of steel piles driven into three different densities of sandy soil; loose, medium and dense. Different types of model piles with different aspect ratios were tested. The results showed that the ultimate pile capacity increases in parallel with an increase in soil density and plug length ratio (PLR). In light of these test results, the authors created an empirical equation to predict the pile bearing capacity of open-ended steel piles based on the percentage of the incremental filling ratio (IFR).

Despite many investigations highlighting the use of artificial neural networks to simulate pile bearing capacity and corresponding settlement, to date, there are still gaps in the subject knowledge. The current study has been conducted to address a gap in the geotechnical literature by carrying out an experimental load carrying capacity study, conducting comprehensive statistical analysis, and developing and training a new, self-tuning, evolutionary neural network algorithm with five input parameters. These parameters can easily be determined without the need for expensive, environmentally unfriendly and time consuming, in-situ testing.

2. Aim and objectives

The current investigation has been performed to address gaps in the geotechnical literature through providing a full comprehensive study in relation to accurate the determination of pile load-settlement curve, the specific objectives are to:

- Carry out experimental pile load-tests to examine the bearing capacity of concrete piles having three pile slenderness' ratios (lc/d), where lc is the effective pile length and d the pile diameter, penetrated in three, relative sand densities (Dr); loose, medium and dense.
- Establish an accurate laboratory database to develop and train the proposed LM algorithm.

- Utilise a new MATLAB training algorithm, i.e. the Levenberg-Marquardt (LM), to develop a predictive model of pile settlement.
- Perform a comprehensive statistical analysis to identify the most influential model input parameters by determining ('Beta' value), to mark the contribution of each parameter by calculating the statistical significance factor ('Sig' value), and to evaluate the reliability of the studied investigation by checking the presence of outliers, data size, data normalisation, and multicolinearity, using SPSS-23 package.
- Hypothesis testing (T-tests and F-tests) has been conducted to establish how representative the database sub-division, training, validation and testing are, with respect to each other.

3. Materials and methods

3.1. Sand properties

The sand utilised in the testing programme is obtained from local supply. It has a relatively negligible impurity level with a quartz (SiO_2) content at 98%. According to the scanning electronic microscopy (SEM) test, the sand were composed of surrounded particles (see Figure 1). The sand can be classified, according to the sand classification criteria stated by the Unified Soil Classification System (USCS), as poorly graded (SP). The coefficient of uniformity (Cu) and the curvature coefficient (Cc) are, respectively, 1.786 and 1.142. The model piles were tested in three densities of sand measuring of loose (18%), medium (50%), and dense (80%), as this represented the entire range of the in situ sand density. The minimum and the maximum sand unit weight was 15.33 kN/m^3 and 17.5 kN/m^3. The soil-pile interface friction angle for loose, medium, and dense sand were 22.6°, 26°, and 30°, respectively. In addition, the sand-sand angle of internal friction for the for loose, medium, and dense sand were 29.5°, 34°, and 40°. The physical properties of the sand samples have been determined through laboratory tests as per the standard methods recommended by the BSI (BS EN 1377:1990). To maintain the impact of the grain size distribution on the combined soil-pile interaction, the ratio between the effective diameter of pile to the medium diameter (d_{50}) of the sand specimen should be 45 (Nunez et al. 1988). In an attempt to minimise the scale factor influence and to give a precise simulation of the sand-pile interaction, it has been suggested by Remaud (1999) that the ratio should be 60 times the diameter of the pile. Taylor (1995) however, proposed that minimum ratio between the aforementioned parameters must not be less than 100. In this study, the ratio of the diameter of the pile to medium diameter (d/d_{50}) is about 133.4 as shown in Figure 2. Thus, the geotechnical scaling standard condition has been met. It is noteworthy that a tube delivery system has been used to arrange the loose sand bed (Schawmb 2009). The end of the system was repeatedly held at a maximum set

distance of about 40 mm between the surface test bed and the sand delivery tube. Moreover. An air pluviation technique has been utlised to prepare the required sand bed (Ueno 2000). The required sand density was controoled by the falling rate at about 800 mm above the sand surface with an accuracy of ±30 mm until the tested depth being achieved. In addition, the dense sand beds were carefully prepared following the procedure detailed by Nasr (2013).

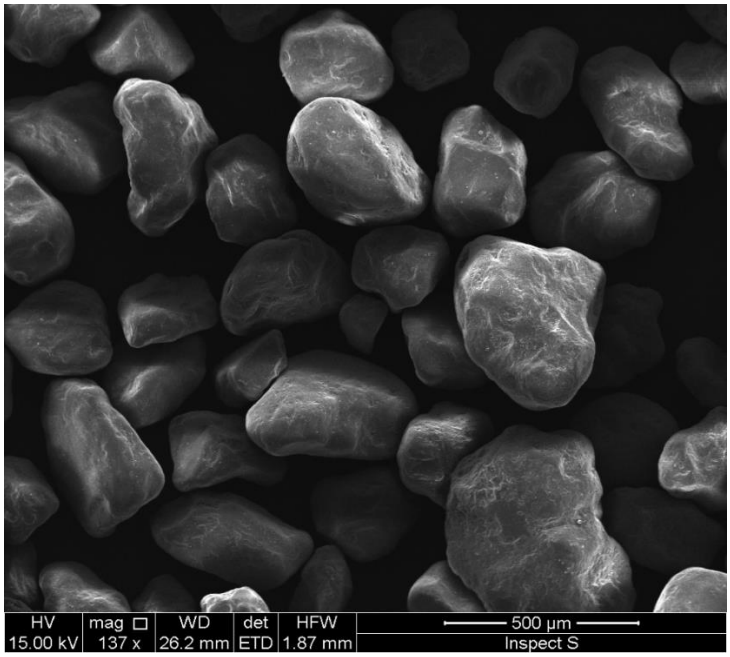

Figure 1. Scanning Electronic Microscopy (SEM) image of the sand specimen.

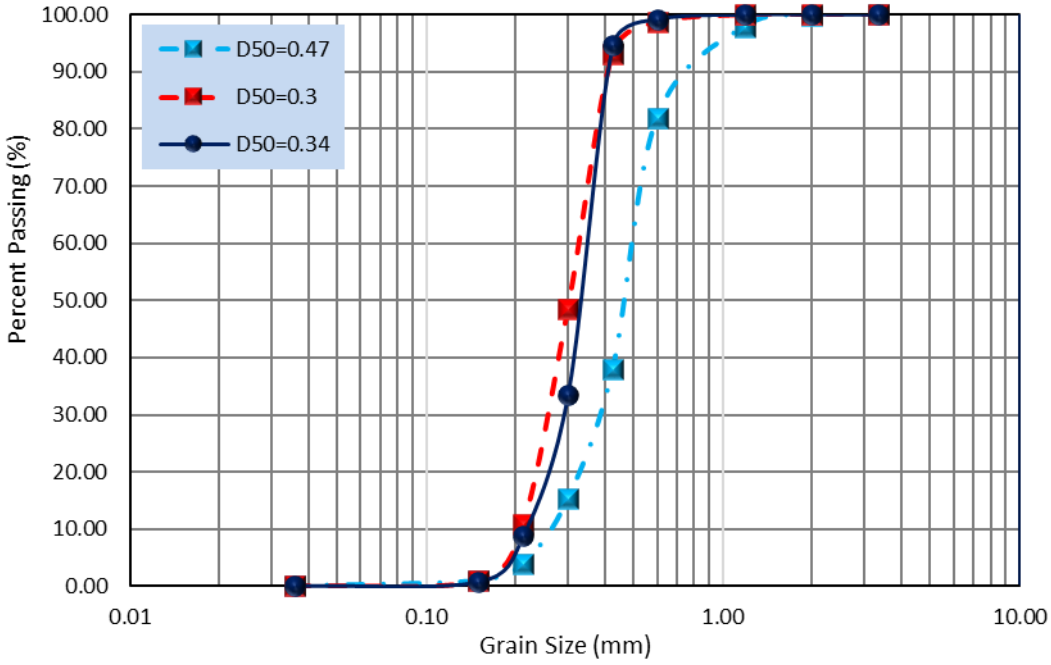

Figure 2. Grain size distribution curves for the sand samples.

3.2. Pile models and loading procedure

Experimental pile load-tests was performed by the authors on square concrete piles with 40 mm diameter using calibrated pile testing chamber (Figure 3). The effective embedment length-to-diameter ratios of 12, 17 and 25 were used to examine the response of rigid and flexible piles (Reddy and Ayothiraman 2015). The concrete pile was characterised by a Poisson's ratio of $\nu = 0.2$ and a Young's modulus of $E = 25$ GPa (Gere and Timoshenko 1997). The pile point of loading was 50 mm above the sand surface to minimise contact of the soil with the pile cap. This can help ensure that the pile capacity is only due to soil-pile interaction. For the mechanical applied load of the pile, a maintained load test was run at loading rate of 1mm/min as recommended by Bowels (1978) and within the limits stated by BSI (BS EN 8004:1986). The compression loads were applied in increments using a new hydraulic jack system connected at the top to a load cell type (DBBSM) having a maximum capacity of 10 kN which was secured between the pile head loading system and the hydraulic ram. Moreover, the loads were applied directly on an aluminium pile cap with dimensions of 25 mm thick and 150 mm diameter. A spherical steel ball bearing was used on the top of the pile cap to avoid eccentricity during the load application. It should be highlighted that the pile load tests were performed at 1 G conditions. Therefore, there will be some differences, due to low effective stress, compared to full-scale tests. Thus, the tests results are limited to low effective over burden pressures. The pile head displacement was monitored using a data acquisition system with 16-bit resolution

instrumented with two linear variable differential transformers (LVDTs) of very high resolution 0.01mm with 150 mm travel to record the corresponding settlement. Using magnetic stands, the LVDTs were placed on the top of the pile cap in pairs so that effect of bending could be accurately accounted for.

Figure 3. Schematic view and dimensions of test configuration.

4. The Levenberg-Marquardt (LM) algorithm model development

The LM training algorithm is a data driven computing method, which, more specifically, succinctly able to correlate inversely and numerically the relationships between set of individual input variables and outputs via

their characteristic mathematical topology (Ahmadi et al. 2015; Nguyen-Truong and Le 2015). It is worth to be noted that the LM consist of three main components: (i) the input layer, (ii) hidden layers and (iii) an output layer(s) (Bashar 2013). Those layers form the artificial neural network (ANN) means of learning and detailing the patterns controlling the dataset that the network is constructed with. The objective of the hidden layer is to transform the model input parameters into the output layer, multiplied by connection weights and any bias either added or subtracted. The aforementioned themes were followed by dividing the gathered experimental dataset into two subsets, named as testing and training. Running the optimisation of interconnected biases and weights was continued until a certain measuring performance indicator was met as described in the following sections. In this study, the Levenberg-Marquardt (LM) algorithm was trained using the multi-layer back propagation (MLBP) method with training parameters, as shown in Table1. The LM training procedure is clearly illustrated in the following design chart (Figure 4).

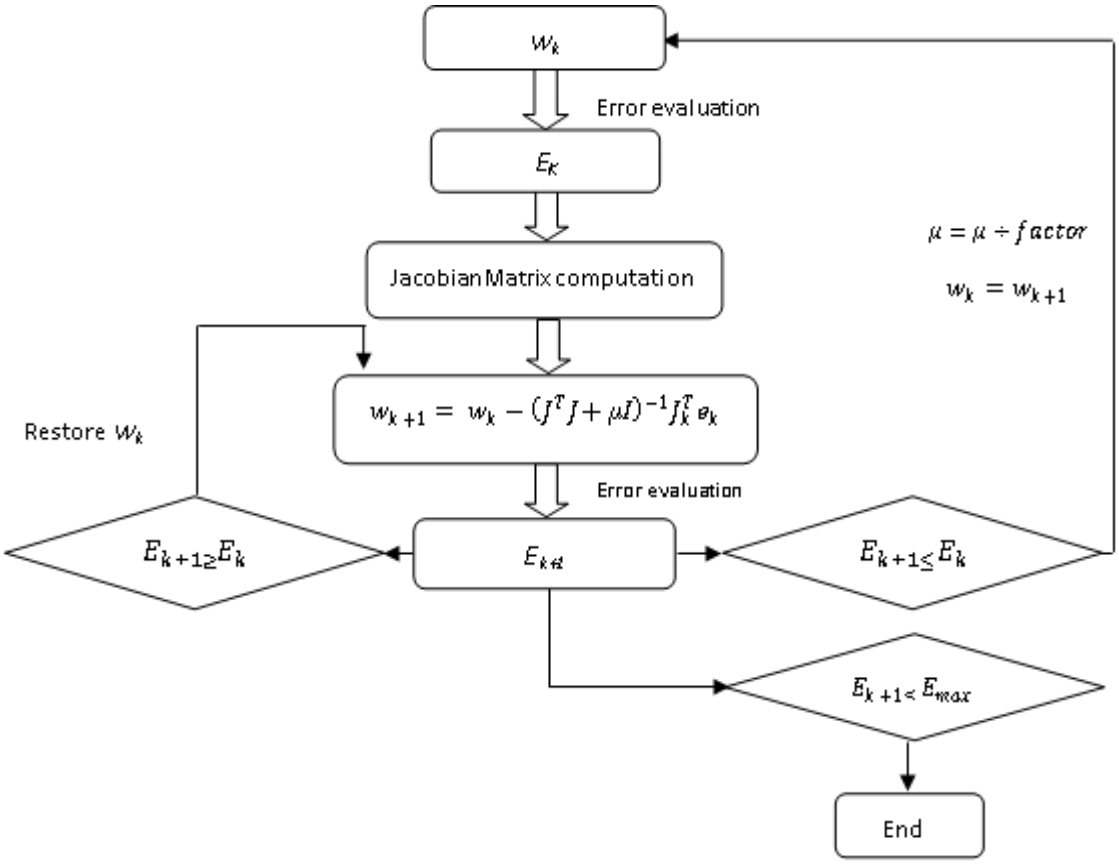

Figure 4. Block diagram shows the training process utilising Levenberg Marquardt (LM) algorithm.

in which w_k represents the existing (initial) connection weight, w_{k+1} is the subsequent connection weight, $E_{k+1} and\ E_k$ are the current and last total error, correspondingly.

Table 1. The Levenberg-Marquardt (LM) training parameters.

Parameter	value	description
net.trainParam.epochs	1000	Maximum number of epochs to train
net. trainParam.goal	0	Performance goal
net. trainParam.Ir	0.01	Learning rate
net. trainParam.Ir_inc	1.05	Ratio to increase learning rate
net. trainParam.Ir_dec	0.7	Ratio to decrease learning rate
net. trainParam.max_fail	6	Maximum validation failure
net. trainParam.max_perf_inc	1.04	Minimum performance increase
net. trainParam.mc	0.9	Momentum constant
net. trainParam.min_grad	1e-5	Minimum performance gradient
net. trainParam.show	25	Epochs between displays (NaN for no displays)

4.1 Statistical significance of each independent variable (IV)

The level of contribution of each independent variable (IV) to the dependent variable (DV) in the constructed model has been ascertained by calculating the relative importance, or Beta value, and the statistical significance (p value). It should be stated that the statistical analysis model has been developed utilising the Multiple Regression (MR) method, as this technique possesses the ability to investigate the complex relationship within a set of variables (Pallant 2005). Any IV at $p > 0.05$ can be discounted as it has no substantial influence on the model target (Field 2008; Hashim et al. 2017b). Statistically, the closest to one the absolute Beta value is, the more significant the impact of that IV on the model (Pallant 2005; Hashim et al. 2017a). Table 2 shows that the applied load (P) and the sand-pile interface friction angle (δ) have the highest contribution to the model output at Beta values of 0.787 and 0.613 respectively. Pile slenderness ratios (lc/d), flexural rigidity (EA), and pile length (lc) made a lessor contribution to the model output. Moreover, results of Table 2 also revealed that the maximum Sig value for all variables is less than 0.05, matching the statistical criteria. Based on the statistical analyses, the LM algorithm has been trained with five parameters, these being applied load, pile slenderness ratio, pile axial rigidity, pile effective length, and the interface friction angle. The model output was pile settlement as illustrated in Figure 5. A summary of the statistical parameters for the training, testing and validation dataset, are given in Table 3.

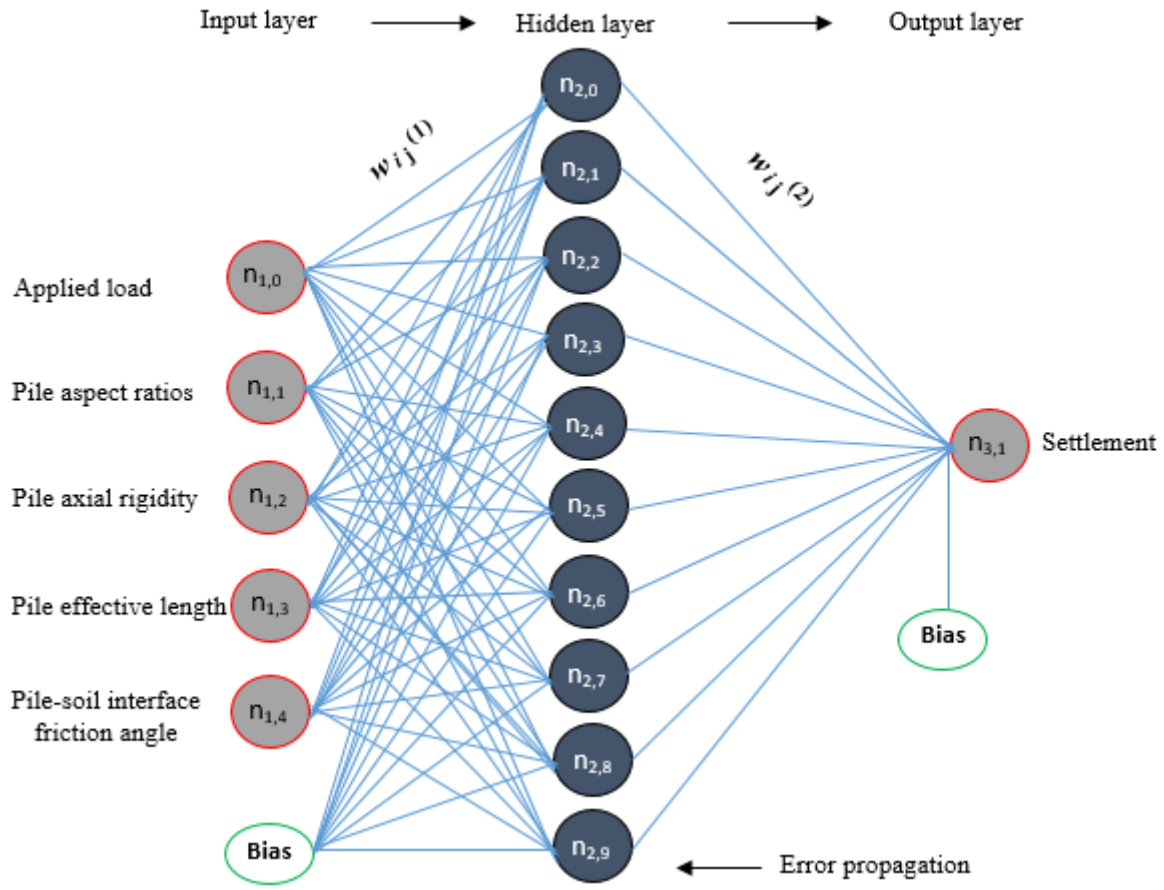

Figure 5. Representation of a typical multilayers feedforward ANN model with one hidden layer.

4.2 Outliers

Outliers can be illustrated as points, or a single data point, that appears to be incompatible with other dataset observations (Walfish 2006). The performance and the generalisation ability of the developed model can be highly influenced by the presence of such extreme points (Hashim et al. 2017b). Therefore, all IVs and DVs should be screened before the training process. The presence of outliers can be tested by determining the Mahalanobis distances (MDs) following the statistical criteria reported by (Tabachnick and Fidell 2013). In this investigation, for five IVs, the screening test revealed that the maximum MDs is 20.52. Whereas, for the experimental dataset, the highest MDs was found to be 10.26 as given in Table 2, which evidences the absence of the outliers.

4.3 Dataset size

The reliability of the size of the dataset must be precisely calculated in order to develop the best relationship between the independent variables (IVs) and the model output, and to obtain an efficient model performance (Pallant 2005; Hashim et al. 2017b). For the five input parameters, according to the equation below, the minimum

dataset size required to train the LM algorithm is 90 (Tabachnick and Fidell 2013). In this paper, there were 254 experimental dataset points used to run the LM training algorithm, satisfying the aforementioned statistical criteria.

$$N > 50 + 8 * IVs \quad (1)$$

Where *N* and *IVs* denote the required size of the sample and number of independent factors to perform the LM training algorithm and to develop a reliable predictive model.

4.4 Multicollinearity

The existence of multicollinearity within the dataset, which negatively influences the performance of the proposed model, cam be clearly pronounced when high correlation exist between IVs (Tabachnick and Fidell 2013). This phenomenon, therefore, could be detected by calculating the value of tolerance, using Equation (2), given by O'brien (2007), where tolerance values of higher than 0.1 indicate the absence of the multicolinearity in the observation being studied (O'brien 2007). In this study, based on the statistical results (Table 2) the existence of multicollinearity in the observation dataset is unanticipated as the tolerance values for all IVs are higher than critical value.

$$Tolerance\ value = 1 - R_i^2 \quad (2)$$

in which R^2 indicates the coefficient of correlation.

Table 2. Results of the statistical analysis.

IVs	Sig. value	Beta. value	Tolerance	Maximum detected MDs
Applied load, (P)	0.000	0.787	0.21	19.26
Sand-pile angle of interface friction, (δ)	0.000	0.613	0.32	
Flexural rigidity, (EA)	0.010	0.02	0.41	
Slenderness ratio, (lc/d)	0.020	0.139	0.75	
Pile effective length, (lc)	0.000	0.101	0.87	

Table 3: Statistical characterisation of testing, training, and validation dataset.

Data Set	Statistical Parameters	Input Variables					Output
		Load (kN)	Slenderness ratio Lc/d	Pile length, (m)	Pile axial rigidity, EA (MN)	Sand-pile friction angle, δ°	Settlement , (mm)
Training Set	Max.	6.78	25	1	251.2	30.1	14.41
	Min.	0.001	12	0.48	47.2	22.8	0.002
	Mean	2.13	17.28	0.72	196.7	26.26	6.14
	S.D.*	1.85	1.34	0.21	90.44	1.11	4.52
	Range	6.78	2.08	0.52	204	7.3	14.41
Testing Set	Max.	6.67	25	1	251.2	30.1	14.21
	Min.	0.001	12	0.48	47.2	22.8	0.003
	Mean	1.83	1218.62	0.70	192.9	25.40	6.25
	S.D.*	1.93	5.53	0.22	93	1.128	4.52
	Range	5.67	13	0.52	204	7.3	14.2
Validation Set	Max.	6.73	25	1	251.2	30.1	14.30
	Min.	0.131	12	0.48	47.2	22.8	0.065
	Mean	2.39	18.06	0.68	189.27	26.32	7.13
	S.D.*	1.94	1.348	0.22	94.64	1.12	4.19
	Range	6.6	13	0.52	204	7.3	13.23

*Standard deviation

4.5 Pre-processing and data classification

To construct the Levenberg-Marquardt (LM) based-ANN model architecture, smooth and to eliminate overfitting, the database is randomly classified into three sets: training, validation and testing. The goal of the training dataset is to create the most appropriate ANN network and fit the model by selecting the optimum unit weight (W_{ij}) and biases (b_{ij}) during the process of training, while the testing set is piloted to deliver an independent check of network performance during the training process. The task for the validation set is to finally evaluate the generalisation ability of the ANN model via using unseen data subset after selecting the appropriate network weights and biases, (Ahmadi et al. 2015; Shahin 2016). The database was normalised between 0.0 and 1.0 before introducing them to the training and generalisation of the network, to eliminate the influence of one factor over another and also to allow each individual variable (IV) to receive the same attention during the training process (Majeed et al. 2013; Jebur et al. 2017). It is crucial that the dataset used for the training, testing and cross validation represent similar populations (Masters 1993). However, statistical analysis, the T-test and F-test, were conducted as shown in Table

4, for normalised data to ensure that the training, cross validation and testing datasets have similar statistical parameters.

Table 4. T-test and F-test results for the (ANN) model inputs and output.

Variable and Data Set	T-value	Lower Critical Value	Upper Critical Value	T-test	F-value	Lower Critical Value	Upper Critical Value	F-test
Load (kN)								
Testing	-0.39	-1.97	1.97	acceptable	1.01	0.68	1.56	acceptable
Validation	0.43	-1.97	1.97	acceptable	1.07	0.68	1.56	acceptable
Slenderness ratio Lc/d								
Testing	-0.81	-1.97	1.97	acceptable	0.93	0.68	1.56	acceptable
Validation	1.26	-1.97	1.97	acceptable	0.88	0.68	1.56	acceptable
Pile length, (m)								
Testing	-0.88	-1.97	1.97	acceptable	0.92	0.68	1.56	acceptable
Validation	1.10	-1.97	1.97	acceptable	0.90	0.68	1.56	acceptable
Pile axial rigidity, (EA)								
Testing	0.33	-1.97	1.97	acceptable	0.95	0.68	1.56	acceptable
Validation	0.58	-1.97	1.97	acceptable	0.91	0.68	1.56	acceptable
Soil-pile friction angle, δ								
Testing	-0.33	-1.97	1.97	acceptable	0.95	0.68	1.56	acceptable
Validation	0.58	-1.97	1.97	acceptable	0.91	0.68	1.56	acceptable
Settlement, (mm)								
Testing	0.86	-1.97	1.97	acceptable	1.37	0.68	1.56	acceptable
Validation	-1.54	-1.97	1.97	acceptable	1.22	0.68	1.56	acceptable

5. Results and discussion

5.1. Architecture and ANN model performance

The ANN was trained with multilayers back propagation technique utilising the Levenberg-Marquardt (LM) MATLAB algorithm version R2017a, as it is a more reliable and a faster approach than all other artificial neural approaches (Jeong and Kim 2005). To include full details about the LM algorithm is beyond the scope of this study but can be found in Hagan et al. (1996). The mean square error (MSE) function was identified to measure the model performance with an error goal set at minimum. According to the referred standards, the TANSIG transfer function (TF) was utilised between layer one and two, while the PURELIN transfer function was used to interconnect layer two and three as shown in Equations (3 and 4), and as recommended by Alizadeh et al. (2012).

The experimental dataset, a total of 254 data points, was randomly divided into three subsets, composed of 70% training (178 data points), 15% testing (38 data points), and 15% validation (38 data points). This division of data is in accordance with standard methods used to develop and train an ANN model (Stojanovic et al. 2016; Morfidis and Kostinakis 2017). The target for the training dataset is to optimise the parameters of the model (the synaptic connection weight (W_{ij}) and bias (b_j)) in order to minimise the percentage of error between the target and predicted values (Alkroosh and Nikraz 2014). The testing subset was piloted to evaluate the generalisability of the trained model. The testing dataset was not used for training; it is to be used assess the generalisability of the algorithm (Millie et al. 2012). The cross-validation sub-set is used to measure the performance of the trained network, and to terminate the process of learning at the minimum error value of the mean square error (MSE) (Tarawneh 2017), as shown in Figure (6). After training the ANN network, the results revealed that the optimum ANN model consisted of three layers; the input layer with five nodes, one hidden layer with 10 neurons and an output layer with one node. At the end of the training course, the final configuration of the proposed LM algorithm is 4-4-1. As mentioned previously, the performance of the LM algorithm was characterised by the mean square error (MSE) as shown in Equation (5). The main objective of the training dataset is to learn the patterns presented in the dataset by updating ANN biases and weights (Ismail et al. 2013). This training process normally ends when the error value is sufficiently small enough (Yadav et al. 2014). The performance of the trained network under training is displayed in Figure 6, the results revealing that the minimum square error (MSE) was 0.0025192 at an epoch of 215. It can also be seen that the training process stopped to avoid overfitting once the cross-validation error started to increase. The variation in error gradient, the Marquardt adjustment parameter (m_u) and checks of the validation are presented in Figure 7. It can be seen that the gradient error is considerably minimised during the training course at 0.004691, while the m_u factor and the validation check numbers are 1e-06 and 6 at an iteration of 221, respectively.

The error histogram graph (EHG) has been presented in Figure 8 to obtain additional verification of network performance. EHG can also give an indication of outliers and data features where the fit is significantly poorer than the majority of the rest of the data (Yadav et al. 2014; Abdellatif et al. 2015). In plot 8, the red, green and the blue bars signify testing, validation and training data, respectively. It should be noted that the majority of data coincide with a zero error line, which represents a scheme for outline verification to determine if the dataset is inadequate.

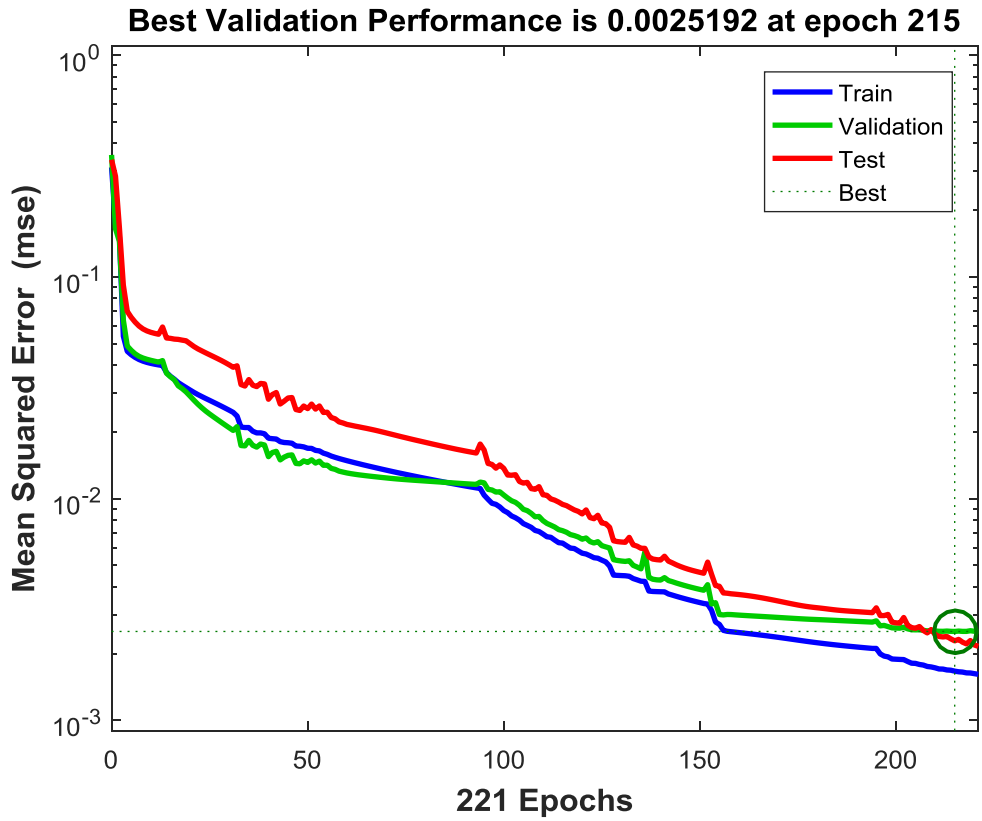

Figure 6. Graph presenting the optimum mean square error (MSE) selected during the training process.

$$Z_j = \frac{1}{1 + \exp\ (\sum_1^n \pm w_{ij}^{(1)}\ x_i \pm\ b_j^{(1)})} \tag{3}$$

$$y = \sum_1^n w_j^{(2)}\ \ z_j\ \pm\ b^{(2)} \tag{4}$$

$$MSE = \frac{1}{n}\left(\sum_1^n (measured(ij) - predicted(ij))^2\right) \tag{5}$$

where the factors b_j (1) and w_{ij} (1) are the biases and weights from the input and output (hidden) layers respectively. b_i (1) and b_i (2) are the bias for layers one and two, *MSE* is the mean square error and *n* is the number of the model input parameters.

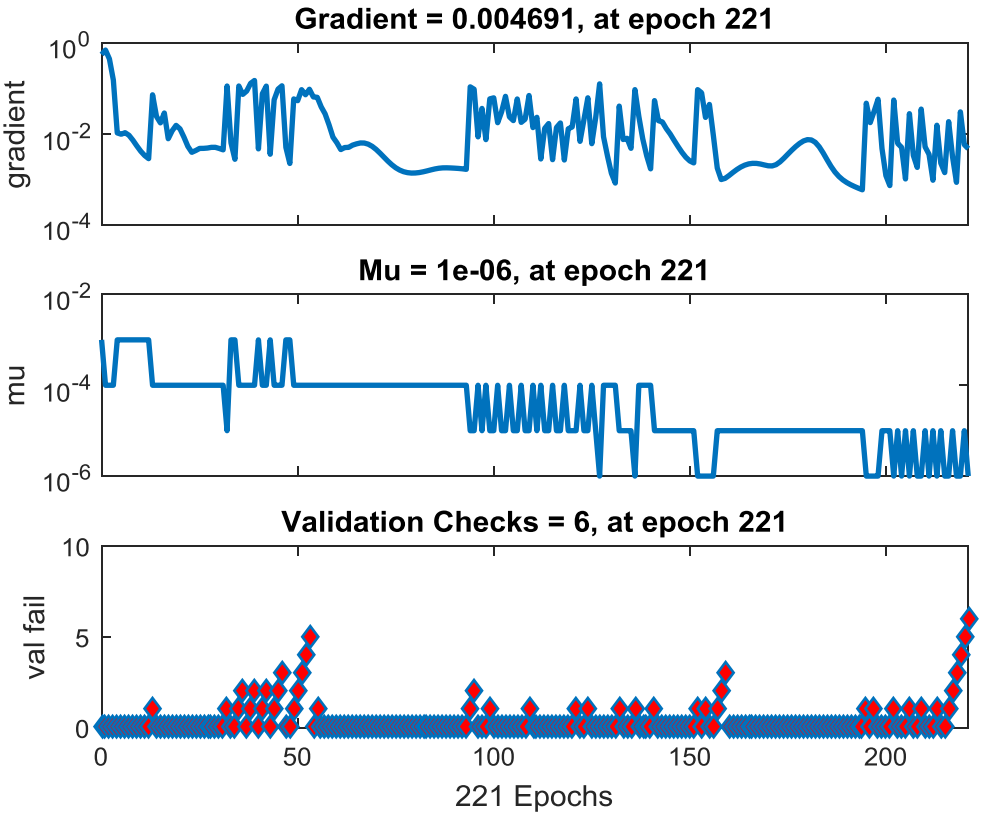

Figure 7. Performance diagrams for the ANN trained network.

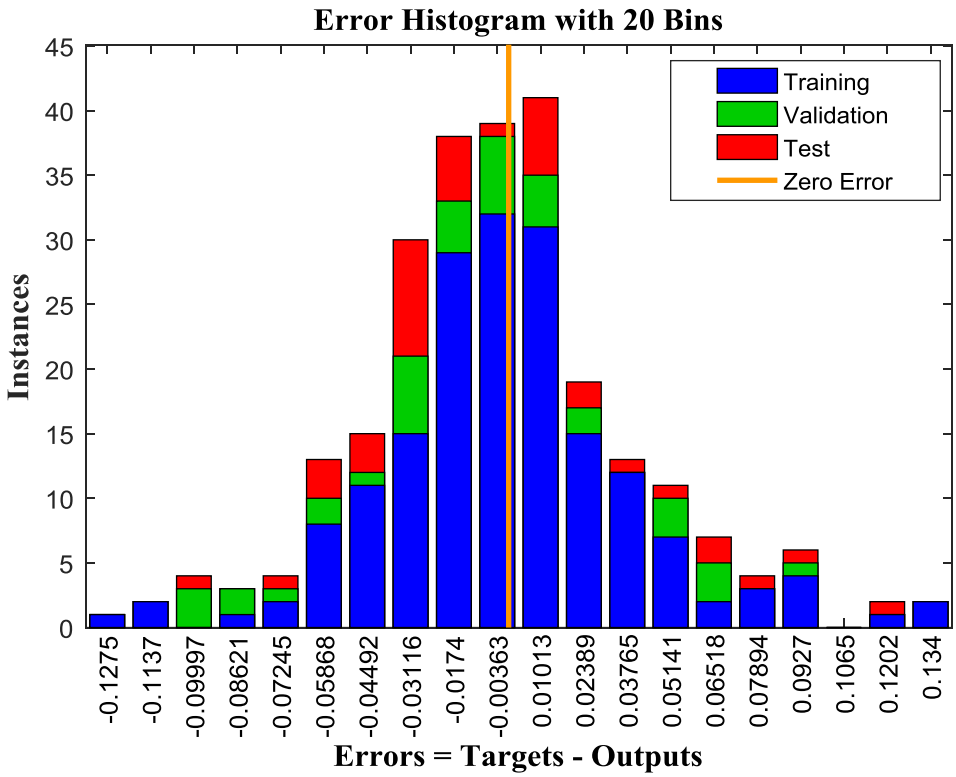

Figure 8. Error histogram during training, testing and validation.

5.2. Evaluation of the robustness of the ANN model

The results of the experimental load-settlement (Q-S) tests and the predicted ANN based outputs are discussed in this section. A series of experimental pile load tests were performed on model concrete piles. The testing program consisted of three piles with slenderness ratios (lc/d) of 12, 17 and 25 where lc is the effective pile depth with diameters of 40 mm to examine the behaviour of rigid and flexible piles. In total, 254 points recorded the experimental pile load test data using a P3 strain indicator as stated previously. Figures 9, 10 and 11 show the distributions of the measured versus predicted load carrying capacity. As depicted, the results revealed the mobilised pile bearing capacity increases with increases in the sand stiffness and the pile effective depth. Plastic mechanisms in the soil surrounding the pile is the leading cause for the non-linearity of the load-settlement curve (Loria et al. 2015). The results shown that an elastic response ca be clearly pronounced in the initial steps from running the pile load test when the pile settlements are less than 1% of pile diameter. Furthermore, for pile driven in loose sand (Figure 9), the influence of soil yielding for applied load higher than 350, 600, and 700 N for lc/d = 12, 17, and 25 can be clearly pronounced where non-linearity is marked. The plots also revealed that as the axial applied loads increase, the behaviour of piles increase in nonlinearity due to the presence of the plastic mechanism within the contacted soil in the effective stress zone. Figures 11 and 12 characterise the load-settlement distribution curves of pile embedded in medium and dense sand. Similarly, a noticeable elastic branch can be realised at early stages of the mechanical applied load. in addition, as the load increases, the response of foundation become more nonlinear until reaching a maximum pile capacity of 10% of pile diameter BSI (BS EN 8004:1986). According to the graphical comparisons, for loose sand, the predicted results are slightly underestimated the pile load-test curves in case of pre-yield working settlement. Moreover, there was an excellent fit between the proposed LM training algorithm and targeted values in post-yield pile load tests responses (often the most important component part for practicing geotechnical engineers), with a coefficient of determination of 0.99008, thus it can be rightly drawn the conclusion that the applied LM training algorithm is a superior method to predict pile load-settlement distribution curves with remarkable accuracy.

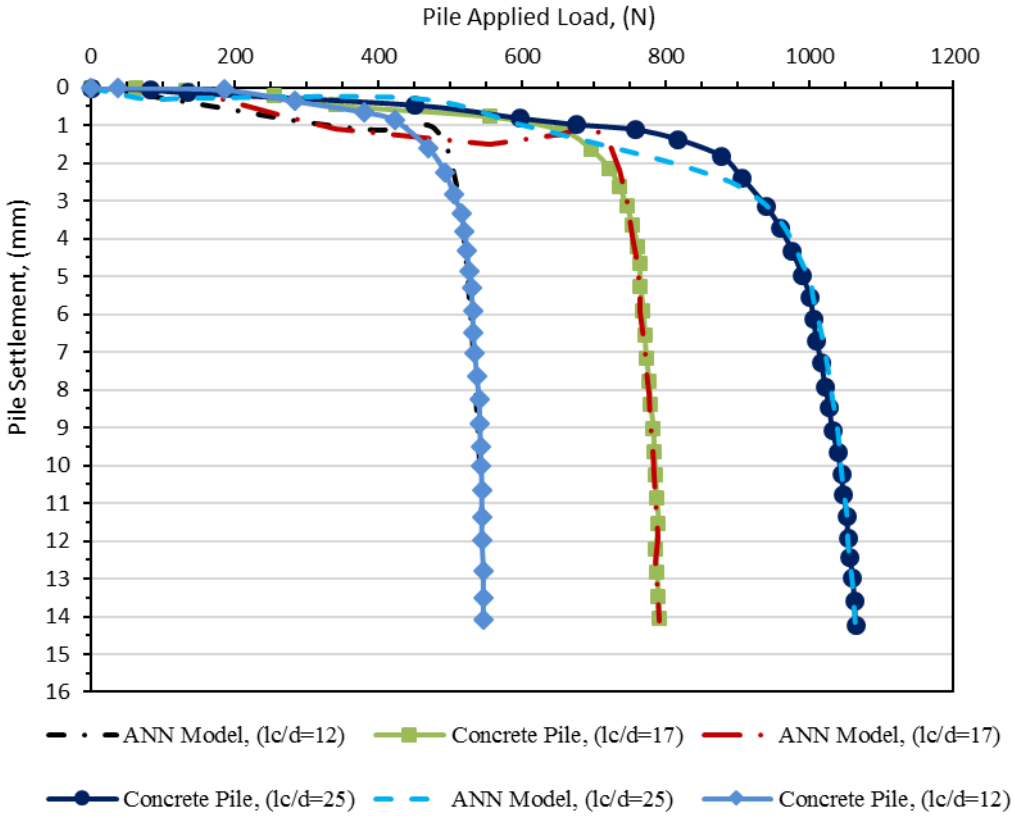

Figure 9. Profiles of measured versus predicted pile load tests for model piles embedded in loose sand.

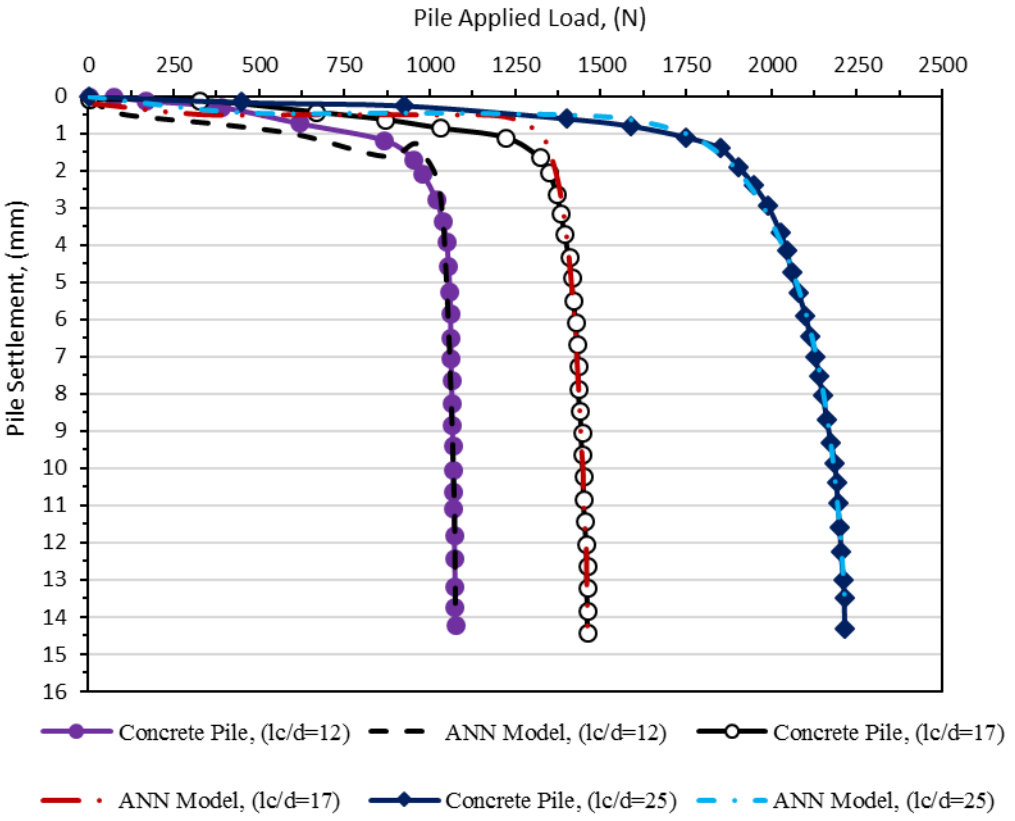

Figure 10. Profiles of measured versus predicted pile load tests for model piles embedded in medium sand.

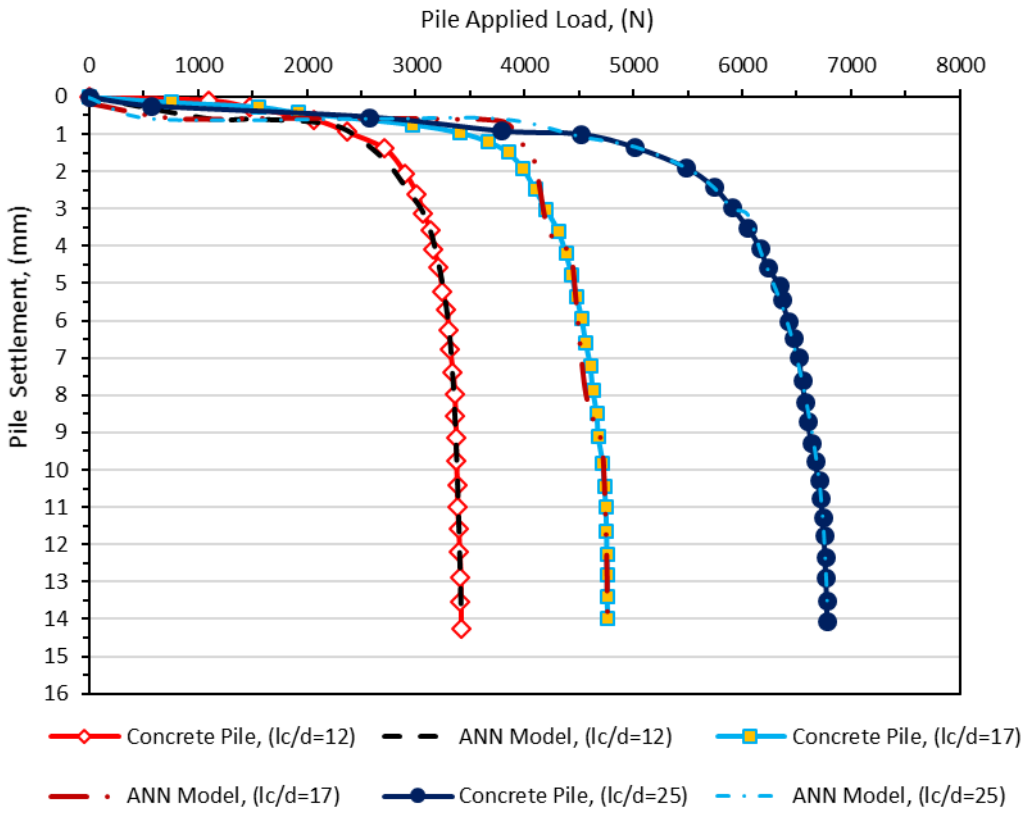

Figure 11. Profiles of measured versus predicted of pile load tests for model piles embedded in dense sand.

The regression calibration curve for the training, testing and validation of all datasets to compare target and predicted settlements values, is illustrated in Figure 12. As demonstrated, the strong capability of the trained algorithm to fully capture the pile settlement is clear. The points in all subdivisions (training, testing and validation) are located close to the best equality line with high measuring performance indicators of 0.99139, 0.98565, 0.98819 and 0.9908, for training, validation, testing of all data, substantiating the application of the LM algorithm as an efficient predictive tool with high accuracy.

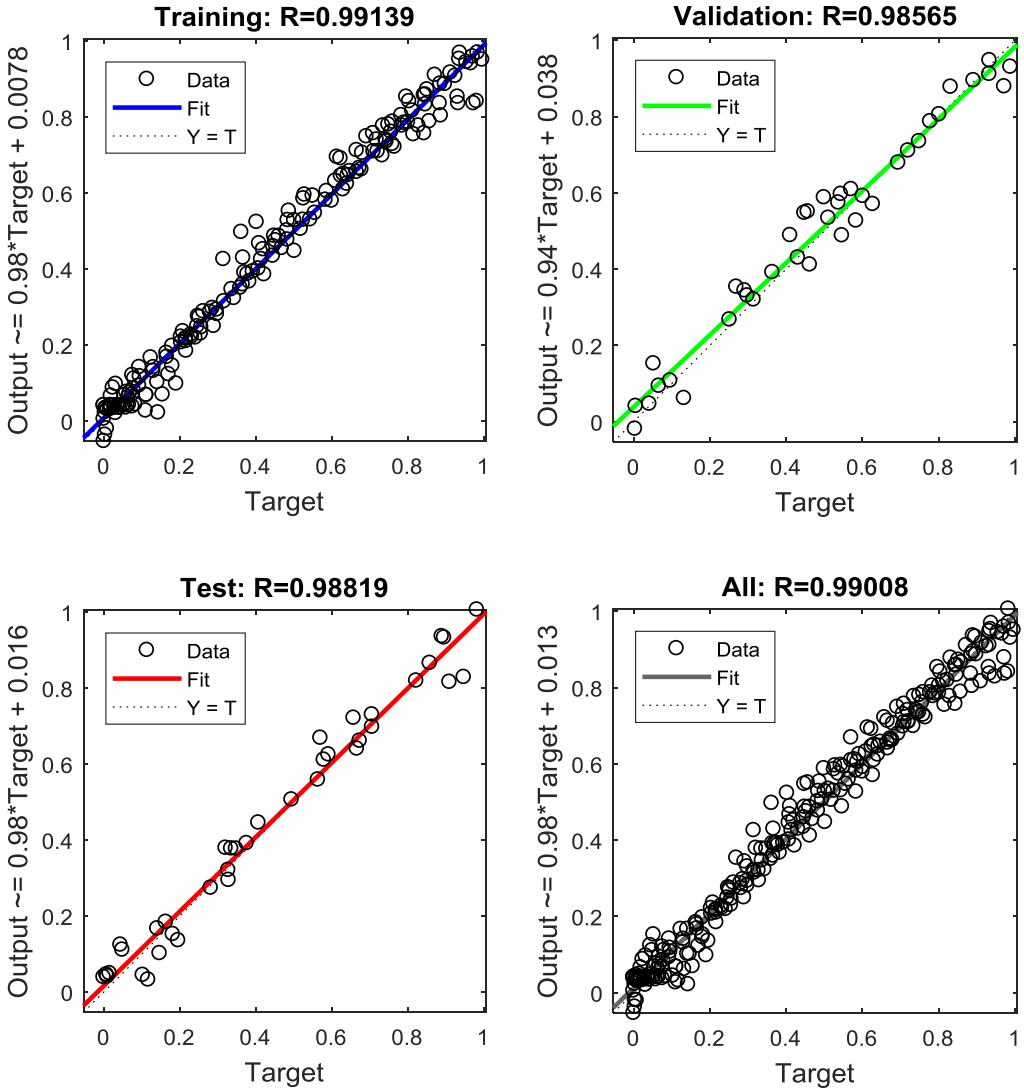

Figure 12. Regression profiles of network-yielded versus measured settlement for the training, testing and validation of all data.

Lastly, the performance of the LM algorithm is further examined graphically using validation dataset, as demonstrated in Figure 13. The vlidation dataset were used to plot a regression calibration curve between targetted versus predicted values, with a 95% confidence interval (CI). Significant agreement can be observed between the measured versus predicted values and it has the lowest scatter around the best equality line at an angle of 45°. This in parallel with a root mean square error (RMSE) and correlation coefficent (R) of 0.0478 and 0.988, which also confirms that the trained network, has the required level of efficiency to reproduce the results of the experimental pile settlement with continuous accuracy.

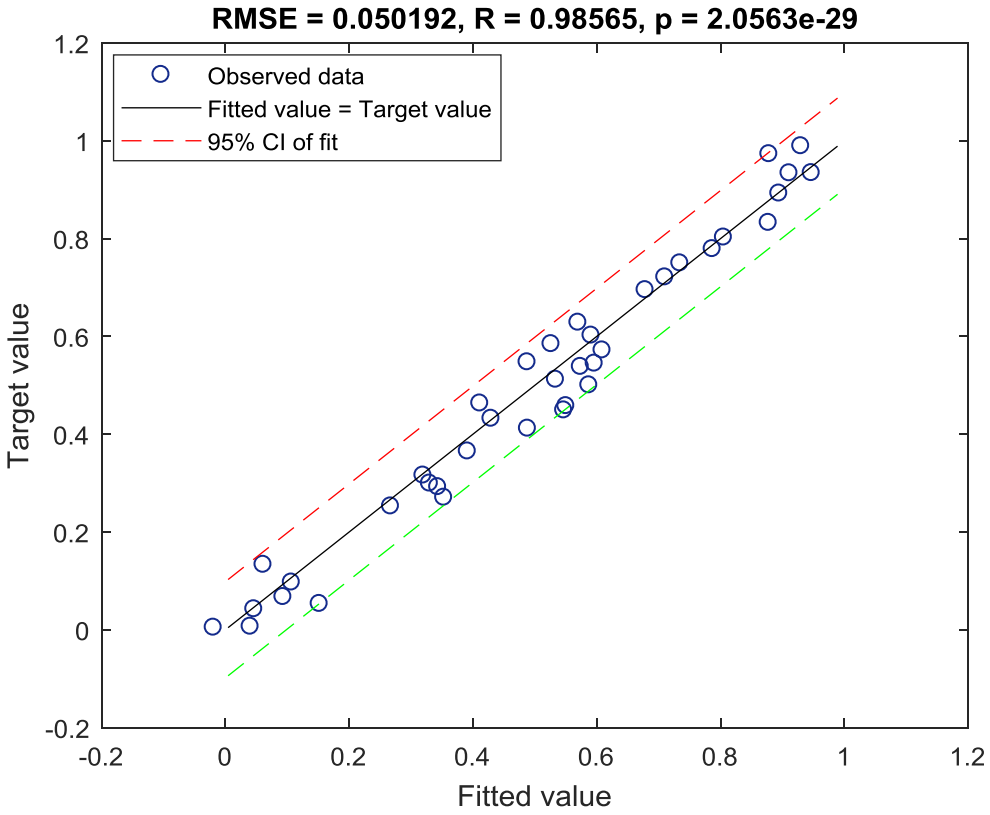

Figure 13. Calibration plot of resulting model for the validation dataset at a 95% confidence interval (CI).

6. Scale factor

Based on the geotechnical scaling criteria stated by Wood (2004), and with consideration of the boundary influence, Equation (6) can be used when the soil stiffness modulus in the radial effective zone of the sand container and in the site (full scale) is identical.

$$E_m I_m = \frac{1}{n^4} E_p I_p \tag{6}$$

where EmIm refers the model pile modulus of elasticity (GPa) and moment of inertia (m^4), respectively, EpIp is the modulus of elasticity and moment of inertia for the prototype pile and n^4 is the scaling factor. The model pile diameter is 40 mm and having different slenderness ratios as reported previously. The dimensions for the range of the prototypes piles were chosen as 300 mm diameter, with 12000 mm length for concrete piles. The flexural rigidity, E for both the concrete model pile and the prototype where chosen to have the same value 25 GPa (Gere and Timoshenko 1997). Based on Equation 6, the scale factor, (n) for prototype concrete pile is 10.6, 14 and 18.5, correspondingly.

7. Outline of the existing pile load-settlement prediction models

In this part of the study, the currently utilised approaches of predicting pile load-settlement is outlined. In addition, comparisons have been made between the experimental results, the proposed optimum ANN model and its prediction performance, and the predicted pile settlement values outlined by the most traditional methods including: Poulos and Davis (1980); Vesic (1977) and Das (1995). As stated previously, the testing data subset was allocated to investigate the predictive ability of the LM based ANN training algorithm. However, the testing data subset was utilised in in this comparison to evaluate the superiority of the LM training algorithm with the aforementioned traditional methods.

7.1. *Poulos and Davis (1980) Approach*

Poulos and Davis (1980) stated the following empirical equations could be used to predict pile settlement for model piles subjected to axial load (Equations 7 and 8):

$$s = \frac{PI}{E_s D} \tag{7}$$

$$I = I_0 R_k R_h R_v \tag{8}$$

in which P, E_s and D stand for pile-applied load, soil modulus of elasticity and diameter of pile, respectively. I is the influence factor of a rigid pile settlement, which involves the layer effect of soil depth, pile compressibility and Poisson's ratio. R_h is the influence factor for finite-depth and R_υ is the Poisson's ratio correction factor. Such factors can be determined from design charts recommended by Poulos and Davis (1980). In this approach, for a rigid pile driven in a semi-infinite soil with 0.5 Poisson's ratio, I_0 is the only influence parameter needing consideration (Baziar et al. 2015).

7.2. *Vesic (1977) Method*

Vesic (1977) suggested that pile settlement could be determined from the summation of three components s_1, s_2 and s_3 using the following simplified formulas (Equations 9, 10 and 11):

$$S_1 = \frac{(P_{wp} + \xi P_{ws})L}{A_{tip}E} \quad (9)$$

$$S_2 = C_p \frac{P_{wp}}{dq_p} \quad (10)$$

$$S_3 = C_s \frac{P_{ws}}{Lq_p} \quad (11)$$

P_{wp} is the working load applied at the pile head, P_{ws} is the load supported by the skin resistance and **ξ** is the skin friction distribution influence factor. C_p is an empirical factor. The coefficients q_p and C_s can be determined through the following equations:

$$q_p = 40\frac{N_{tip}l}{d} \leq 400N_{tip}(kPa) \quad (12)$$

$$C_s = \left(0.93 + 0.16\sqrt{\frac{l}{d}}\right)C_p \quad (13)$$

The factor **ξ** can be assumed to equal 0.5 and the parameter C_p is equal to 0.09 (Poulos and Davis 1980).

7.3. Das (1995) Method

The method proposed by Das (1995) is the similar as that proposed by Vesic (1977) with some modifications in calculating S2 and S3. These modifications can be precisely summarised by the following equations:

$$S_2 = \frac{P_{wp}D}{A_{tip}E_s}(1 - \upsilon^2)I_p \quad (14)$$

$$S_3 = \left(\frac{P_{ws}}{Ol_{penetarted}}\right)\left(\frac{d}{E_s}\right)(1 - \upsilon^2)I_{ps} \quad (15)$$

$$I_{ps} = 2 + 0.35\sqrt{\frac{l_{penetrated}}{d}} \quad (16)$$

where I_p is equal to 0.88 as recommended by Poulos and Davis (1980).

With the intention of further exploring the validity and to quantify the efficiency of the trained ANN model, Figure 14, describes a graphical comparison between the predicted results using the LM training algorithm, the experimental pile load test for piles with aspect ratios of 12, 17 and 25, and the pile-load settlement estimated by the most conventional methods use in the absence of the in-situ load carrying capacity test, as described previously. The comparative results indicated that pile settlement predicted using the LM training algorithm are in good agreement with the fitted line, suggesting that the application of LM based ANN optimal model as a high-precision with obvious advantages.

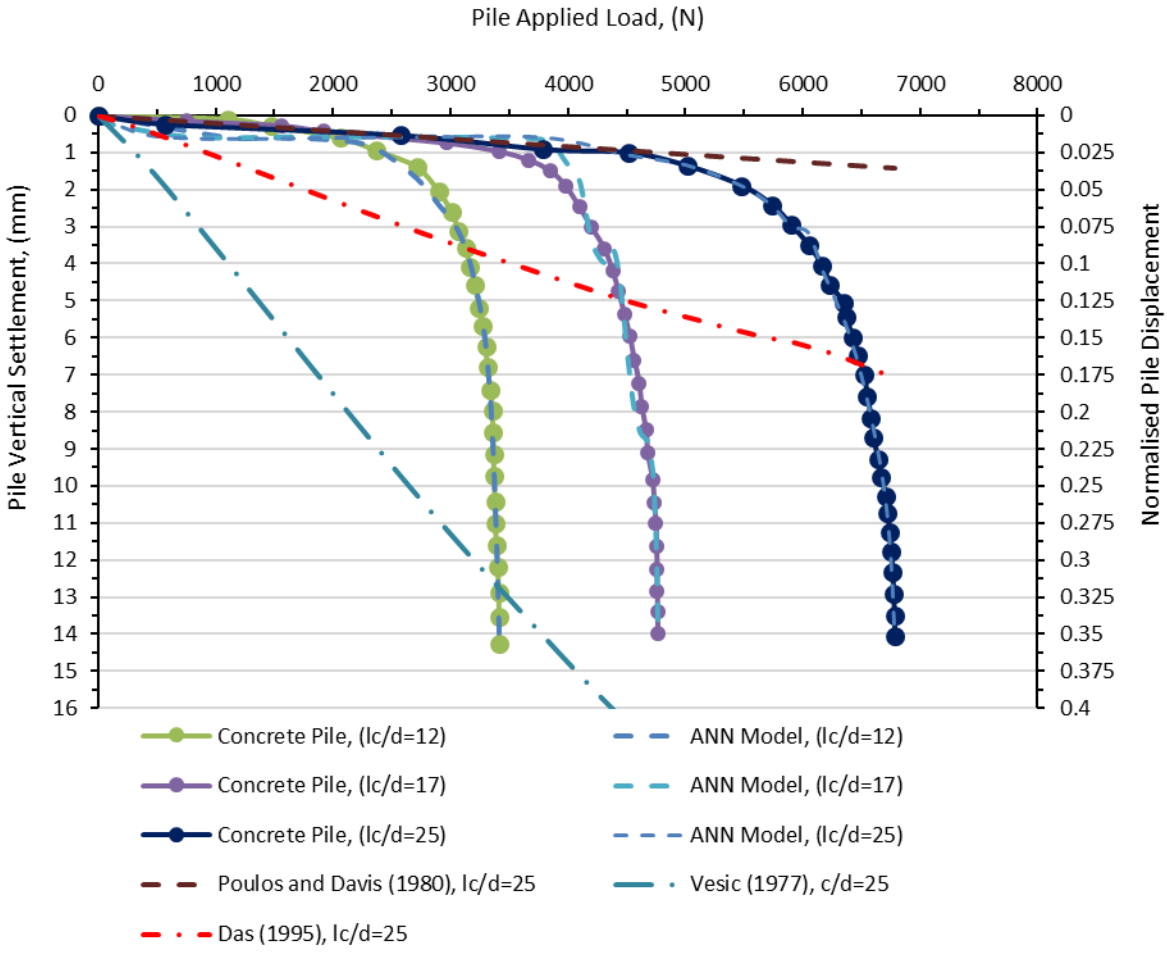

Figure 14. Profiles of measured versus predicted pile load-settlement for the proposed LM compared with other conventional methods.

8. Conclusions

A series of expermental studies have been conducted to examine the pile bearing capacity of concrete piles embeded in sandy soil with three relative densites of sand, ranging of loose, medium, and dense. Accoring to the statistacal parameters, the applied load, P, sand-pile friction angle, δ are the most significant independent variables (IVs), whereas, pile axial rigidity, EA, pile slenderness ratio, (lc/d), pile effective length, lc, were identified as being less responsible for pile settlement. In addition, the results of the screening dataset test reveals that the maximum MDs is less than the critical value (20.52) for five individual variables, which confirms the absence of outliers in the experimental dataset. The LM training algorithm has favorable features such as simplicity, high efficiency, ease of application and generalisation capability, which makes it an attractive choice to capture highly non-linear load-settlement responses. In essence, based on the results of the graphical comparison of pile carrying capacity and the regression calibration curve, the proposed algorithm can be used as an efficient data-driven approach to accurately model pile settlement with a root mean square error (RMSE), correlation coefficient (R) and mean absolute error (MAE) of 0.050192, 0.98819 and 0.0025192, respectively. One of the advantages of the proposed method is that pile load settlement response can be successfully simulated using the proposed LM algorithm, with five input parameters that can be easily determined without the need to perform expensive and time consuming tests, which demonstrated the feasibility of the proposed method in future applications.

Acknowledgements

The authors would like to thank the reviewers for their constructive feedback, which help to improve the quality of the paper. The authors are extremely grateful to all organisations that funded the study described in this paper, which was supported by the Iraqi Ministry of Higher Education and Scientific Research and University of Wasit.

References

Abdellatif M, Atherton W, Alkhaddar R, Osman Y. 2015. Flood risk assessment for urban water system in a changing climate using artificial neural network. J, Nat Hazards 79:1059–1077.

Ahmadi MA, Zendehboudi S, Dusseault MB. 2015. Evolving simple-to-use method to determine watereoil relative permeability in petroleum reservoirs. Petroleum, 2:67-78.

Alizadeh B, Najjari S, Kadkhodaie-Ilkhchi A. 2012. Artificial neural network modeling and cluster analysis for organic facies and burial history estimation using well log data: A case study of the South Pars Gas Field, Persian Gulf, Iran. J. Comput and Geosci 45:261-269.

Alkroosh I, Nikraz H. 2014. Predicting pile dynamic capacity via applicati on of an evolutionary algorithm. Soils andFoundations (54):233-242.

Alkroosh IS, Bahadori M, Nikraz H, Bahadori A. 2015. Regressive approach for predicting bearing capacity of bored piles from cone penetration test data. J. of Rock Mecha and Geotech Eng, 7(5):584-592.

Bashar T. 2013. Pipe pilesetup:Databaseandpredictionmodelusingartificial neural network. Soils andFoundations, 53(4):607-615.

Baziar MH, Azizkandi AS, Kashkooli A. 2015. Prediction of Pile Settlement based on Cone Penetration Test Results: An ANN Approach. KSCE J. of Civil Eng, 19(1): 98-106.

Bowels JE. 1978. Engineering properties of soils and their measurement. 2nd ed. New York (NY): McGraw-Hill International. Book Company:213.

BSI. BS EN 1377:1990. Methods of test for soils for civil engineering purposes. BSI, London, UK.

BSI. BS EN 8004:1986. Code of practice for foundations. BSI, London, UK.

Das BM. 1995. Principles of foundation engineering, third edition. Boston ua PWS Publ. Co.

Das BM. 2015. Principles of Foundation Engineering, eighth edition. United State of America: Global Engineering, Nelson Education LTD.

Doherty P, Spagnoli G, Doherty M. 2015. Laboratory investigations to assess the feasibility of employing a novel mixed-in-place offshore pile in calcareous deposits. Ships and Offshore Structures:1-11.

Ebrahimian B, Movahed M. 2016. Application of an evolutionary-based approach in evaluating pile bearing capacity using CPT results. Ships and Offshore Structures, 12(7):937-953.

Elsayed T, El-Shaib M, Gbr K. 2014. Reliability of fixed offshore jacket platform against earthquake collapse. Ships and Offshore Structures, 11(6):167-181.

Fattah MY, Al-Soudani WH. 2014. Bearing Capacity of Closed and Open Ended Pipe Piles Installed in Loose Sand with Emphasis on Soil Plug. Indian Journal of Geo-Marine Science, 45(5):703-724.

Fattah MY, Al-Soudani WH. 2016. Bearing capacity of open-ended pipe piles with restricted soil plug. Ships and Offshore Structures 11:501-516.

Fattah MY, Al-soudani WH, Omar M. 2016. Estimation of bearing capacity of open-ended model piles in sand. Arab J Geosci, 9(242):1-14.

Field A. 2008. Multiple regression using SPSS. Res. Methods Psychol. C8057:1-11.

Gere JM, Timoshenko SP. 1997. Mechanics of materials xvi, 912 p. 4th eddition

Hagan MT, Demuth HB, Beale MH, Jesús OD 1996. *Neural Network Design*.

Hagan MT, Menhaj MB. 1994. Training feedforward network swiththe Mar- quardt algorithm. IEEETrans. NeuralNetwork, 5:989–993.

Hashim KS, Shaw A, Al Khaddar R, Pedrola MO, Phipps D. 2017a. Energy efficient electrocoagulation using a new flow column reactorto remove nitrate from drinking water - Experimental, statistical, and economic approach. J. of Environ Manag 196:224-233.

Hashim KS, Shaw A, AL Khaddar R, Pedrola MO, Phipps D. 2017b. Iron removal, energy consumption and operating cost of electrocoagulation of drinking water using a new flow column reactor. J. of Environ Manag, 189:98-108.

Ismail A, Jeng D-S, Zhang LL. 2013. An optimised product-unit neural network with a novel PSO-BP hybrid training algorithm: applications to load deformation analysis of axially loaded piles. Engineering Applications of Artificial Intelligence 26(10):2305-2314.

Ismail A, Jeng DS. 2011. Modelling load settlement behaviour of piles using high-order neural network (hon-pile model). Engineering Application of Articiacl Intelligence, 24(5):813–821.

Jaeel AJ, Al-wared AI, Ismail ZZ. 2016. Prediction of sustainable electricity generation in microbial fuel cell by neural network: Effect of anode angle with respect to flow direction. J. of Electroan Chemis, 767:56-62.

Jebur AA, Atherton W, Alkhadar RM, Loffill E. 2017. Piles in sandy soil: A numerical study and experimental validation. Procedia Engineering 196:60-67.

Jebur AA, Atherton W, Alkhaddar RM, Loffill E. 2016. Simulation of Soil-Pile Interaction of Steel Batter Piles Penetrated in Sandy Soil Subjected to Pull-Out Loads. International Conference of Civil, Environmental, Structural, Construction and Architectural Engineering 10(5):605-610.

Jeong D-I, Kim Y-O. 2005. Rainfall-runoff models using artificial neural networks for ensemble stream flow prediction. Hydrol Process 19(19):3819–3835.

Kabiri-Samani AR, Aghaee-Tarazjani J, Borghei SM, Jeng DS. 2011. Application of neural networks and fuzzy logic models to long-shore sediment transport. Applied Soft Computing, 11(2):2880–2887.

Kaiser MJ, Snyder BF. 2014. Offshore wind structure weight algorithms. Ships and Offshore Structures, 9(6):551-556.

Loria RAF, Orellana F, Minardi A, Fürbringer J, Laloui L. 2015. Predicting the axial capacity of piles in sand. Comput and Geotech, 69:485-495.

Majeed AH, Mahmood KR, Jebur AA. 2013. Simulation of Hyperbolic Stress-Strain Parameters of Soils Using Artificial Neural Networks. Procedings of the 23rd International Conference on Geotechnical Engineering; Feb 21st - 23rd; Hammamet, Tunisia:105-115.

Masters T. 1993. PracticalNeuralNetworkRecipesinC++. Academic. San Diego.

Millie DF, Weckman GR, Young II WA, Ivey JE, Carrick HJ. 2012. Modeling microalgal abundance with artificial neural networks: Demonstration of a heuristic 'Grey-Box' to deconvolve and quantify environmental influences. Environmental Modelling & Software 38:27-39.

Mohammadi EG, Ashour A. 2016. A feasibility study of BBP for predicting shear capacity of FRP reinforced concrete beams without stirrups. Advances in Engineering Software, 97:29-39.

Momeni E, Nazir A, Armaghani DJ, Maizir H. 2014. Prediction of pile bearing capacity using a hybrid genetic algorithm-based ANN. Measurement, 57:122-131.

Morfidis K, Kostinakis K. 2017. Seismic parameters' combinations for the optimum prediction of the damage state of R/C buildings using neural networks. Advances in Engineering Software 106:1-16.

Nasr AMA. 2013. Uplift Behavior of Vertical Piles Embedded in Oil-Contaminated Sand. Journal of Geotechnical and Geoenvironmental Engineering, 139:162-174.

Nguyen-Truong HT, Le HM. 2015. An Implementation of the Levenberg–Marquardt Algorithm Forsimultaneous-Energy-Gradient Fitting Using Two-Layer Feed Forwardneural Networks. Chemical Physics Letters 629:40-45.

Nunez I, Hoadley P, Randolph M, Hulett J. 1988. Driving and Tension Loading of Piles in Sand on a Centrifuge. In: Corte JF, editor. Centrifuge´ 88. In: Proceding of International Conference Centrifuge. Rotterdam, Paris:353–362.

O'brien RM. 2007. A caution regarding rules of thumb for variance inflation factors. Qual. Quant, 41:673-690.

Pallant J. 2005. SPSS Survival Manual. Allen & Unwin, Australia.

Poulos HG, Davis EH. 1980. Pile Foundation Analysis and Design. John Wiley & Sons, New York, etc.

Reddy KM, Ayothiraman R. 2015. Experimental Studies on Behavior of Single Pile under Combined Uplift and Lateral Loading. Journal of Geotechnical and Geoenvironmental Engineering, 141:1-10.

Remaud D. 1999. Pieux Sous Charges Latérales: Etude Expérimentale De L'effet De Groupe. PhD thesis. Université de Nantes; French.

Schawmb T. 2009. The Continuous Helical Displacement pile in comparison to conventional piling techniques. Masters of Science. University of Dundee.

Schmidhuber J. 2015. Deep learning in neural networks: An overview. Neural Networks 61:85-17.

Shahin MA. 2016. State-of-the-art review of some artificial intelligence applications in pile foundations. Geoscience Frontiers Journal, 7(1):33-44.

Stojanovic B, Milivojevic M, Milivojevic N, Antonijevic D. 2016. A self-tuning system for dam behavior modeling based on evolving artificial neural networks. Advances in Engineering Software 97:85-95.

Sui T, Zhang C, Guo Y, Zheng J, Jeng D, Zhang J, Zhang W. 2016. Three-dimensional numerical model for waveinduced seabed response around mono-pile. Ships and Offshore Structures, 11(6):667-678.

Tabachnick BG, Fidell LS. 2013. Using Multivariate Statistics. Sixth Edition, Allyn and Bacon, Boston.

Tarawneh B. 2017. Predicting standard penetration test N-value from cone penetration test data using artificial neural networks. Geoscience Frontiers 8:199-204.

Taylor RN. 1995. Geotechnical Centrifuge Technology. First ed., Chapman & Hall, London.

Tomlinson MJ, Woodward J. 2014. Pile Design and Construction. Sixth Edution, E & FN Spon, London, U.K.

Ueno K. 2000. Methods for preparation of sand samples Centrifuge. In: Proceedings of the International Conference Centrifuge 98. Tokyo, Japan, Taylor and Francis:23-25.

Vesic AS. 1977. Design of pile foundations. National cooperative highway research program, synthesis of practice No. 42. Washington, DC: Transportation Research Board.

Vu-Bac N, Lahmer T, Zhang Y, Zhuang X, Rabczuk T. 2014. Stochastic predictions of interfacial characteristic of polymeric nanocomposites (pncs). Composites. Part B, Engineering, 59:80–95.

Walfish S. 2006. A review of statistical outlier methods. Pharm. Technol 30:82-86.

Wood DM. 2004. Geotechnical Modelling. Spon Press, Taylor and Francis Group, United States of America.

Xu L-Y, Cai F, Wang G-X, Ugai K. 2013. Nonlinear analysis of laterally loaded single piles in sand using modified strain wedge model. Computers and Geotechnics, 51:60-71.

Yadav AK, Malik H, Chandel SS. 2014. Selection of most relevant input parameters using WEKA for artificial neural network based solar radiation prediction models. Renewable and Sustainable Energy Reviews, 31:509-519.